Available online at www.sciencedirect.com
SCIENCE DIRECT®
Journal of Power Sources 141 (2005) 205–210
JOURNAL OF POWER SOURCES
www.elsevier.com/locate/jpowsour

Current density distribution in PEFC

Zhixiang Liu[a], Zongqiang Mao[a,*], Bing Wu[b], Lisheng Wang[b], Volkmar M. Schmidt[c]

[a] *Institute of Nuclear and New Energy Technology (INET), Room A314, Energy Science Building, Tsinghua University, Beijing 100084, PR China*
[b] *Beijing LN Power Sources Co. Ltd, Beijing, China*
[c] *Institute of Electrochemical Process Engineering, Mannheim University of Applied Sciences, Mannheim, Germany*

Received 16 July 2004; received in revised form 10 September 2004; accepted 1 October 2004
Available online 8 December 2004

Abstract

The determination of the current distribution in a polymer electrolyte fuel cell (PEFC) is of great practical importance to optimize the process parameter such as the flow field design, the humidification of reaction gases and the utilization of the fuel gas. In this paper, subcells approach is used to measure current density distribution in PEFC with an active electrode area of 30 cm^2. Fuel cell performances determined under different operation conditions clearly indicate that the water balance influences the cell performance most significantly. Furthermore, it is interesting to note that under certain condition both membrane drying and electrode flooding are shown simultaneously inducing performance decaying.
© 2004 Elsevier B.V. All rights reserved.

Keywords: Proton exchange membrane; Fuel cell; Current density distribution

1. Introduction

The polymer electrolyte fuel cell (PEFC) is regarded as one of the most promising propulsion systems for the forthcoming age of electric vehicles (EVs), because this system has many benefits such as high power density, quick start-up, low temperature operation and rapid response to loads [1]. In the past years, more and more automotive companies have developed their own PEFC powered demonstration vehicles. While at the same time, there are still many challenges [2] for this technology straightening its way to commercialisation; one of them is the optimization of the current density distribution, which is affected by the following parameters:

– stoichiometries of the fuel gas and oxygen/air;
– humidification conditions;
– microstructure of the gas diffusion electrode (thickness, structure, ionic and electronic conductivity, gas diffusion layer);
– flow field design.

A non-uniform distribution of these parameters within the cell will result in an non-uniform current density distribution leading to lower catalyst utilization, lower energy efficiency and last but not least to a reduced life time of the cell [3]. To measure current density distribution in the fuel cell plane will further contribute to a better understanding of mass transport process in the fuel cell and should lead to an optimized design of the relevant fuel cell components (i.e., gas diffusion electrode with electrocatalyst, membrane electrode assembly with gas diffusion layer, gas manifolding system, bipolar plate).

In the past decade, intensive modeling work on the PEFC single cell has been done by many researchers [4–8]. To evaluate the models, current density distribution measurement experiments have been reported by several groups in parallel.

* Corresponding author. Tel.: +86 10 62784827; fax: +86 10 62771150.
E-mail address: maozq@tsinghua.edu.cn (Z. Mao).

0378-7753/$ – see front matter © 2004 Elsevier B.V. All rights reserved.
doi:10.1016/j.jpowsour.2004.10.003

Los Alamos National Laboratory (LANL) adapted printed circuit board approach to measure local current densities in a PEFC cell. The authors measured current density and high frequency resistance distribution under different operation conditions in a 100 cm^2 fuel cell [3]. Stumper et al. [9] in Ballard Power Systems Inc., compared three approaches for current distribution measurement: partial MEA approach, subcells approach and current distribution mapping approach. Different to Stumper's mapping approach, in which a series of graphite blocks are used, Wieser et al. [10] used Hall sensors to map current density distribution in 600 cm^2 fuel cell. The current distribution mapping methods have high spatial resolution and could give transient distribution information. Noponen et al. [11] used a neilsbed to measure current density in a free-breathing PEFC. Most recently, Mench et al. used segmented anode approach to measure current density distribution in a direct methanol fuel cell (DMFC) [12] and a PEFC [13].

The basic idea for current density measurements is the use of a segmented flow field plate to measure local currents separately. There are some experimental aspects to be noticed in such flow field segmenting method:

(1) It is difficult to make sure that every segment is similarly well contacted with the carbon paper so that all contact resistances are about the same. In Noponen's neilsbed [11], contact resistance difference is shown to affect measurement results greatly.
(2) Gas leakage should be avoided though the gaps between the segments.

In the present work, Stumper's subcells approach [9] is modified to measure current density distribution in a 30 cm^2 PEFC. The segmented anode plate is specially designed to prevent leakage and assure parallelism between the segments.

2. Experimental

2.1. Anode plate

For the measurements of current density distribution, a 20-mm thick copper plate was used for the anode, which is thick enough to make sure that bracing effect will have the least influence in the measurement. Wieser et al. [10] have pointed out that for fuel cell with large active area, bracing condition will have strong effect on current density distribution. In the anode plate, 12 apertures with steps are drilled at proper positions. Then 12 copper bolts, which are insulated to the plate with plastic gaskets are emplaced into the apertures and fastened with nuts. The gaskets also function as leakage proof for gases. Then the working plane of the plate is milled flat and machined with serpentine flow channels. At last this plane is coated with gold to avoid corrosion and reduce contact resistance. The structure of the anode plate could be seen in Figs. 1 and 2. It could also be seen that each circular bolt is designated with a number as seen in Fig. 1.

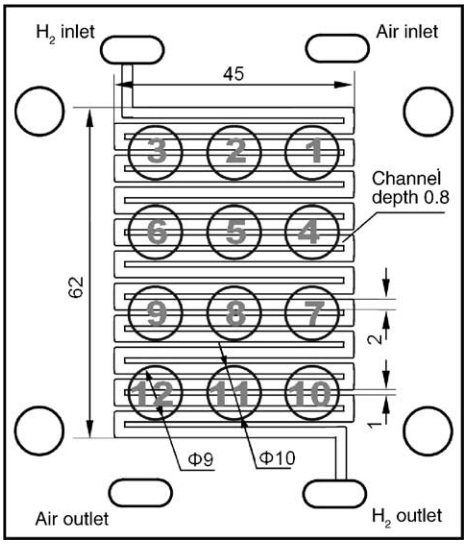

Fig. 1. Structural plot of the anode plate.

2.2. Membrane electrode assembly

The MEA used in our experiments is "01 type" MEA of Beijing LN Power Sources Co. Ltd. with the active area about 30 cm^2 (4.7 cm × 6.4 cm). Here for current distribution measurement, special MEAs are prepared with 12 little segments on the anode side: after the anode carbon paper is painted with catalyst, 12 circular carbon flakes with a diameter of 9 mm are cut down from it, corresponding to the positions of the bolts in the anode plate. The flakes are then cut to 8 mm diameter ones and placed back to the original positions, hot-pressed with a cathode carbon paper and a Nafion® 112 membrane to be an anode-segmented-MEA.

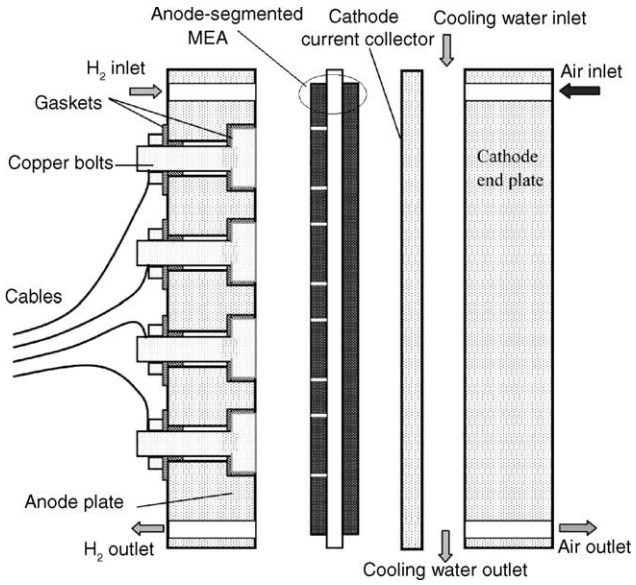

Fig. 2. Schematic of the fuel cell for current distribution measurement.

2.3. Measurement system

For the anode plate, each bolt is connected with a 10-mΩ current-viewing resistor and then connected to the electric load together with the main plate. The measurements were done in the galvanostatic mode applying constant currents through the cell between 0 and 30 A. The voltage of each resistor shared is then recorded, together with the potential of each subcell and the main cell. It could be seen that the subcells are not working on the same potential, which is a little bit different from a real fuel cell. However, the potential difference between each subcell is so small that it will not introduce too much error in results. The difference of the local current densities between the subcells was estimated to be less than 1%. All the experiments were conducted on a fuel cell measurement platform provided by Beijing LN Power Sources Co. Ltd.

3. Results and discussions

3.1. Base case

In the Beijing LN fuel cell test station, normal operation conditions for "01 type" fuel cell are listed in the following:

- pressure of hydrogen and air: 3 bar (absolute pressure);
- humidifying temperature of hydrogen and air: 75 °C;
- cell temperature: 75°C;
- stoichiometric flow ratio of hydrogen and air: 2.

These parameters are regarded as the base case for local current density measurement presented in this paper.

Fig. 3 gives the current density distribution plot of the base case under different applied currents. It can be seen that in the case of lower electronic loads, the current density of the middle area (subcells 4–9) is higher than that of the inlet area (subcells 1–3) and the outlet area (subcells 10–12). While with increasing load the current density of the inlet area increases more rapidly than that of the outlet area. At a total current of 24 A through the cell, the local current in the inlet area is almost twice that of the outlet area.

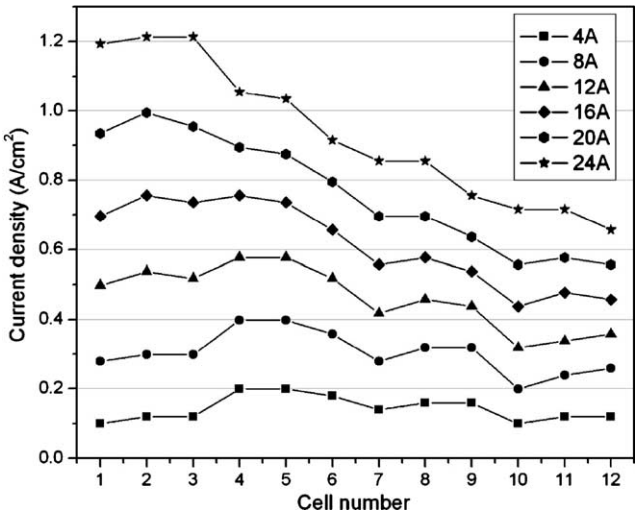

Fig. 3. Current density of the subcells at different total cell currents under base case; $p_{H_2} = p_{air} = 3$ bar; $T_{humid} = T_{cell} = 75\,^{\circ}C$; $\xi_{H_2} = \xi_{air} = 2$.

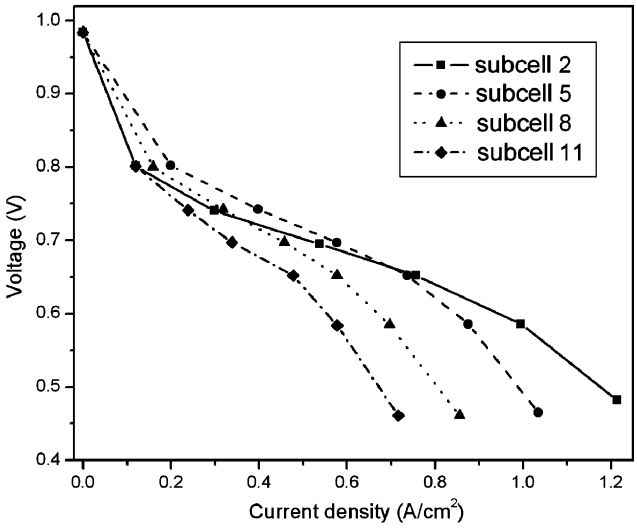

Fig. 4. Current density/cell voltage plots of some subcells under base case; $p_{H_2} = p_{air} = 3$ bar; $T_{humid} = T_{cell} = 75\,^{\circ}C$; $\xi_{H_2} = \xi_{air} = 2$.

Fig. 4 shows the polarization curves of some subcells: 2, 5, 8 and 11. With lower loads, the performance of the inlet area is inferior to that of the middle area. On the other hand, higher loads cause the best performance. This observation indicates that, with lower applied currents produces water amounts in the cell, which might not be enough to hydrate the membrane of the inlet area full sufficiently. While in the middle area, the membrane is very good humidified, because water is produced leading to a better performance. At increasing loads, the feed gases transport enough water to saturate the inlet area. Under these conditions the best performance is obtained. Along the follow channel, with more and more water produced, the MEA is more and more seriously flooded. So subcells nearer to the outlet is easier to be flooded and the polarization curve drops rapidly at lower current density value.

The current distribution results reported in the present paper are different to those in reference [3]. In their results, current density of the middle area is almost the smallest, while the outlet area the highest. Many modeling results give current density decaying trend along the flow channel [14,15], which is very similar to the present results with higher loads. Comparing experimental data presented here with those of Mench et al. [13], the trend is almost the same.

In the following experiment, the fuel cell is operated at a total current of 30 A. After operating for a short time, the voltage suddenly dropped to zero without current dropping. When the air flux is adjusted a much higher values, liquid water droplets could be seen blown out of the cell. Then the voltage reached the normal value. This observation indicates that at high loads, the water produced in the cell could not

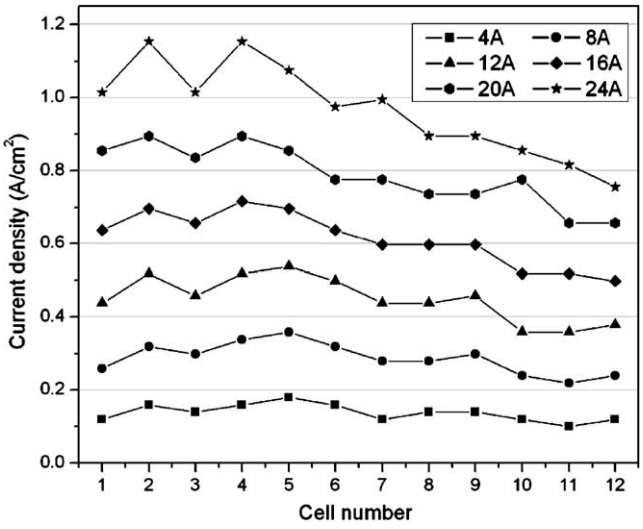

Fig. 5. Current density of the subcells at different total cell currents and lower cell temperature; $p_{H_2} = p_{air} = 3$ bar; $T_{humid} = T_{cell} = 60\,^{\circ}C$; $\xi_{H_2} = \xi_{air} = 2$.

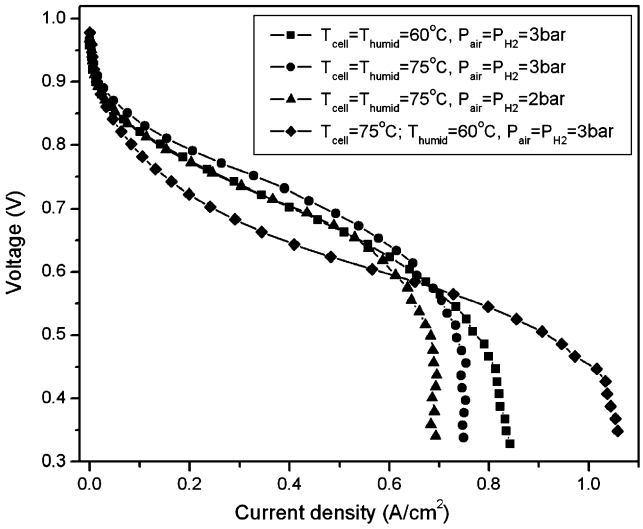

Fig. 6. Current density/cell voltage plots of the fuel cell under different conditions.

be blown out of cell easily. Thus, liquid water accumulates and blocks the pores of the carbon paper, which makes it difficult for oxygen to transport from the flow channel to the catalyst layer. When oxygen concentration on the catalyst surface drops to zero, the oxygen concentration overpotential leads to cell voltage drop down to zero sharply. Since the cell is operated under constant current in these experiments, this could lead to a cell reversal evolving hydrogen instead of oxygen reduction, i.e., electrolysis instead of fuel cell mode.

3.2. Lower operation temperature

When the fuel cell is operated at 60 °C with the same humidifying temperature, similar current density distribution is obtained compared to the base case as shown in Fig. 5. However, current density difference between the inlet and the outlet area is sometimes not as great as the base case. This means that electrode flooding is not so serious compared with the base case. To confirm that, current/voltage curves of the whole cell (including the subcells) are measured under different operation conditions. In this experiment the cell voltage is controlled and was linearly decreased with a scan rate of $1\,mV\,s^{-1}$ and the reactant fluxes are fixed to a value, which was two times the flow ratio of $0.8\,A\,cm^{-2}$. Polarization curves measured under different conditions are plotted in Fig. 6. Comparing the curve of the base case and that of the lower temperature operation, it could be seen that performance is lower at 60 °C than at 75 °C. However, flooding takes place at higher current values. The reason for this might be the lower partial pressure of water vapor is at lower temperature. Thus, under operating conditions of the cell at lower humidifying and reacting temperature, less water is brought into the fuel cell. It is estimated that the air brings about 50% less water into the fuel cell at 60 °C than 75 °C and that there is 12% less water (including humidifying water and produced water) in the fuel cell at 60 °C.

3.3. Lower operation pressure

With the polarization curves in Fig. 6 we can see that the cell performance under 2 bar is inferior to that of the base case, especially for flooding under lower current density value. Fig. 7 demonstrates more unevenly current distribution comparing with Fig. 3. With 16 A load, current density of the outlet area is about half that of the inlet area and difference between them is higher with 20 A load. The reason of the more uneven distribution of current density lies in two aspects: first, about 50% more water is brought into the fuel cell at lower pressure than the base case, so the electrode is more seriously flooded; second, oxygen partial pressure be-

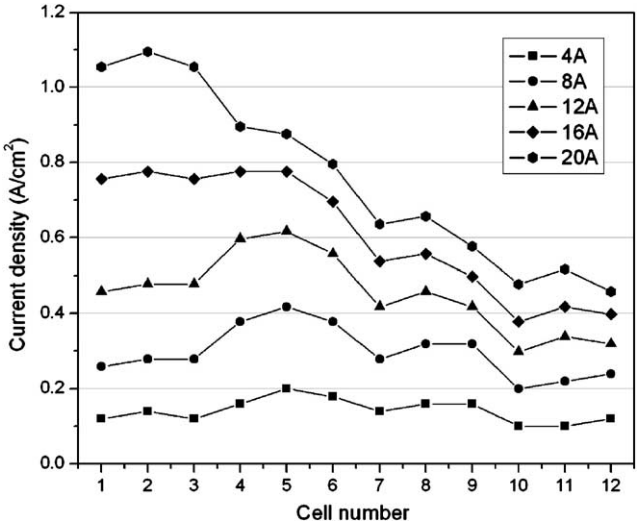

Fig. 7. Current density of the subcells under lower pressure; $p_{H_2} = p_{air} = 2$ bar; $T_{humid} = T_{cell} = 75\,^{\circ}C$; $\xi_{H_2} = \xi_{air} = 2$.

comes lower and lower along the flow channel. With lower partial pressure and heavier flooding, it is more difficult to transport oxygen through the pores of the carbon paper to the catalyst layer. As a result, a more uneven current distribution trend is shown.

3.4. Lower humidifying temperature

The former experiments clearly show that flooding influences the performance of the fuel cell. Along with the flow channel, flooding becomes more important. However, as shown in the former figures, current density of the inlet area is lower than that of the middle area with lower loads. It can be concluded that the inlet area is not fully saturated. To confirm it, the fuel cell is operated at low humidifying temperature. The cell performance given in Fig. 6 reveals at 60 °C humidifying and 75 °C reaction exhibits a much inferior performance compared to the base case at lower current, but it is far less easy to be flooded.

It is interesting to note that under some conditions, both membrane drying and electrode flooding phenomena are apparent regarding the current distribution plots. Fig. 8 shows that with lower loads (up to 16 A), current density increases from the inlet to the outlet area; and with the increasing of load, current density of the outlet area increases quicker than that of the inlet area. With higher loads (more than 16 A), current density of middle area increases rapidly, while that of the outlet area increases much slower. Fig. 9 shows polarization curves of some subcells. It is obvious that, with 60 °C humidifying for the feed gases, the inlet area suffers from membrane drying, which could be deduced from the poor performance of the inlet area shown in Figs. 8 and 9. Because water produced is not too much to flood the electrode with lower loads, membrane saturating condition is becoming better along the flow channel leading to increasing current density. When fuel cell load is high enough, first it

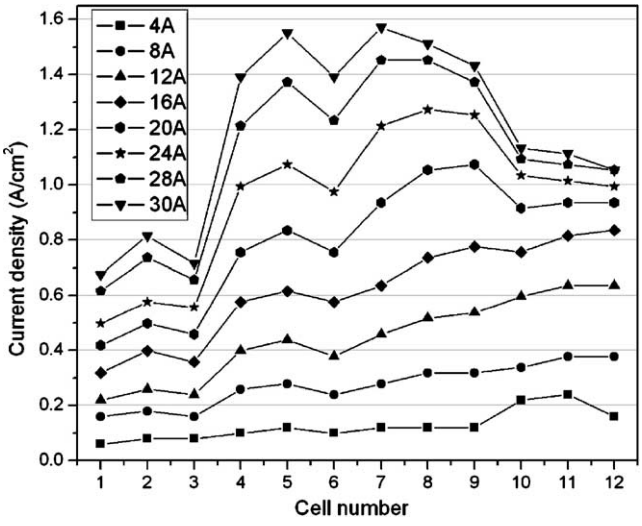

Fig. 8. Current density of the subcells under lower humidifying temperature; $p_{H_2} = p_{air} = 3$ bar; $T_{humid} = 60$ °C, $T_{cell} = 75$ °C; $\xi_{H_2} = \xi_{air} = 2$.

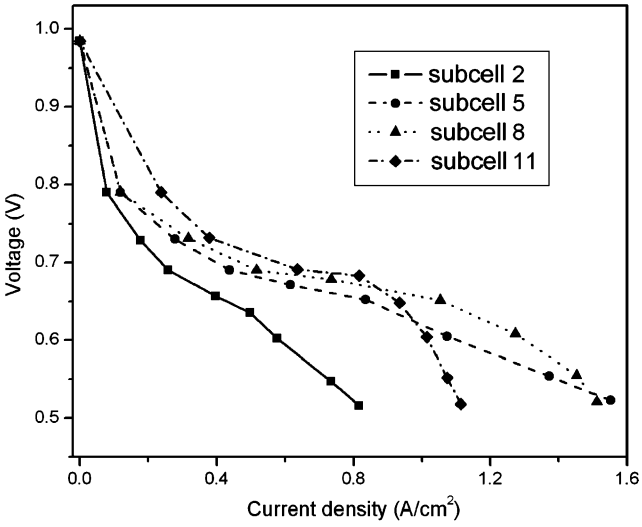

Fig. 9. Current density/cell voltage plots of some subcells under lower humidifying temperature; $p_{H_2} = p_{air} = 3$ bar; $T_{humid} = 60$ °C, $T_{cell} = 75$ °C; $\xi_{H_2} = \xi_{air} = 2$.

is the outlet area that is being flooded by liquid water. Thus, current density does not increase much with the increasing of loads. However, the middle area is very good humidified without serious flooding, so rapid increasing could be seen first for the third row and then for the second row. When the load is higher enough, the flooding area extends to the third row, of which area the current density increasing speed of slows down. Here it could be seen that there is an optimal value for the fuel cell humidified by water: with less water, membrane will not be full saturated and will not show the best performance. On the other hand, with more water, the electrode will be flooded and causes difficulties in gas diffusing.

3.5. Different stoichiometric flow ratio of air

The dependency of the current distribution on the variation of the air stoichiometry is shown in Fig. 10. When the airflow rate was enhanced from 2 to 4 and 6, the current density of the inlet area decreases, while that of the middle area (first the second row and then the third row) and the outlet area increases. For regions in the fuel cell being flooded, higher air flow rate will improve liquid water draining out of the cell and lighten MEA flooding. But for regions without flooding, higher flow rate will speedup membrane drying. For the most inclined drying inlet region, lower flow ratio will help retaining water and avoid drying. For the most inclined flooding outlet region, higher flow ratio will help draining liquid water and alleviate flooding. So there exists an optimal flow rate for the cell performance. This goal can in principle be realized by optimizing the flow field design: for the inlet area, more parallel flow channels are required to slower down the flow rate, favorable for water maintaining; for the outlet region, less flow channels are should speedup the flow rate, favorable for water draining. That is to say, current measurement

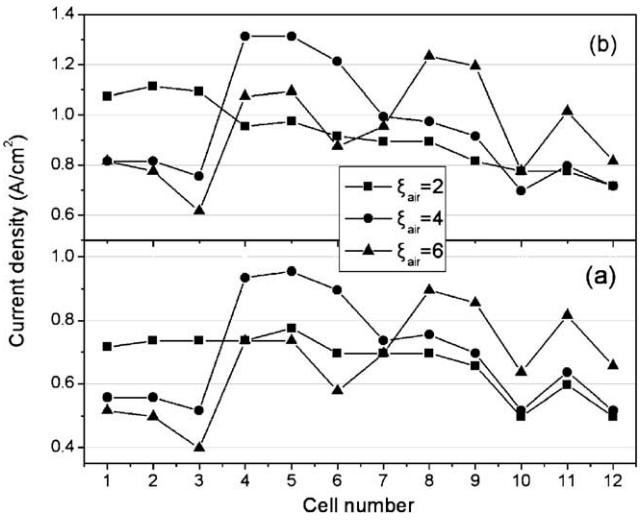

Fig. 10. Current density of the subcells with different stoichiometric flow ratios of air with 12 A (a) and 24 A (b) load; $p_{H_2} = p_{air} = 3$ bar; $T_{humid} = T_{cell} = 75\,^{\circ}C$; $\xi_{H_2} = 2$; $I = 24$ A.

results will give very useful information to guide flow field designing.

4. Conclusion

It was demonstrated that water distribution is the most important and sensitive factor to influence the cell performance of a PEFC. The inlet region is most likely to suffer from membrane drying, while the outlet region is most likely to suffer from electrode flooding. Under certain conditions, these two effects could be seen significantly influencing performance of the fuel cell simultaneously.

Although the current density measurement method presented in this work has given very useful results for fuel cell performance optimization, there are still some problems to be solved:

1) The segments of the anode plate ride on several flow channels, so it is difficult to explain the current difference between the subcells in the same row.
2) Liquid water is likely to accumulate in the cirque regions between the circular flakes and the anode carbon paper, which may introduce some influence.
3) The subcells and the main anode plate are not operated with the same potential value, which is not equivalent to a real fuel cell rigorously.

The future work should be oriented towards:

1) Perfect the measure system with non-segmented MEA and multichannelled potentiostat as demonstrated in [13].
2) Scale the anode plate up to measure MEA with larger area, such as the 02 type MEA (150 cm^2).
3) Current density distribution measurements using different flow field designs should be evaluated to optimize the flow field in the bipolar plate of a PEFC.

Acknowledgements

The authors would like to thank “National 973 Project on Hydrogen Energy (TG2000026410)” and “International Cooperation Project on Hydrogen Energy (2001AA515080)” for financial support of this work. Liu thanks the state of Baden-Württemberg/Germany for a scholarship. V.M.S thanks Daimler Chrysler AG for financial support.

References

[1] V. Mehta, J.S. Cooper, J. Power Sources 114 (2003) 32–53.
[2] P. Costamagna, S. Srinivasan, J. Power Sources 102 (2001) 253–269.
[3] S.J.C. Cleghorn, C.R. Derouin, M.S. Wilson, S. Gottesfeld, J. Appl. Electrochem. 28 (1998) 663–672.
[4] T.E. Springer, T.A. Zawodzinski, S. Gottesfeld, J. Electrochem. Soc. 138 (1991) 2334–2342.
[5] D.M. Bernardi, M.W. Verbrugge, J. Electrochem. Soc. 139 (1992) 2477–2491.
[6] W.S. He, J.S. Yi, T.V. Nguyen, AIChE J. 46 (2000) 2053–2064.
[7] P. Costamagna, Chem. Eng. Sci. 56 (2001) 323–332.
[8] S. Dutta, S. Shimpalee, J.W. Van Zee, J. Appl. Electrochem. 30 (2000) 135–146.
[9] J. Stumper, S.A. Campbell, D.P. Wilkinson, M.C. Johnson, M. Davis, Electrochim. Acta 43 (1998) 3773–3783.
[10] Ch. Wieser, A. Helmbold, E. Gülzow, J. Appl. Electrochem. 30 (2000) 803–807.
[11] M. Noponen, T. Mennola, M. Mikkola, T. Hottinen, P. Lund, J. Power Sources 106 (2002) 304–312.
[12] M.M. Mench, C.Y. Wang, J. Electrochem. Soc. 150 (2003) A79–A85.
[13] M.M. Mench, C.Y. Wang, M. Ishikawa, J. Electrochem. Soc. 150 (2003) A1052–A1059.
[14] T. Berning, D.M. Lu, N. Djilali, J. Power Sources 106 (2002) 284–294.
[15] P.W. Li, L. Schaefer, Q.M. Wang, T. Zhang, M.K. Chyu, J. Power Sources 115 (2003) 90–100.